

Local work function changes determined by field emission resonances: NaCl/Ag(100)

Hans-Christoph Ploigt, Christophe Brun, Marina Pivetta, François Patthey, and Wolf-Dieter Schneider
École Polytechnique Fédérale de Lausanne, Institut de Physique des Nanostructures, CH-1015 Lausanne, Switzerland
 (Received 9 October 2007; published 6 November 2007)

Electrons trapped in field emission resonances (FERs) in front of a Ag(100) surface covered with ultrathin NaCl islands are probed by scanning tunneling spectroscopy. The eigenstates in the potential well formed between the tip and the sample are calculated within a one-dimensional model. This approach permits to locally determine a work function reduction of 1.3 eV in going from the bare substrate to NaCl islands of up to 3 ML. Spatial mapping of the FERs across a NaCl island edge at typical distances of 1 nm from the surface yields a lateral resolution for the surface potential changes of 1 nm.

DOI: [10.1103/PhysRevB.76.195404](https://doi.org/10.1103/PhysRevB.76.195404)

PACS number(s): 73.20.At, 73.21.Ac, 73.21.Fg

The work function ϕ is a fundamental property of any metal surface. It is defined as the minimum energy that is necessary to remove an electron from the metal to infinity at 0 K. Measuring ϕ provides a straightforward method to monitor the state of a surface because any adsorbed species or surface defect will generally induce changes in ϕ . This phenomenon has important consequences concerning reaction mechanisms and catalysis at surfaces because it can promote reactivity.¹ However, the work function value determined by most experimental methods is averaged over large sample areas.^{1,2} This averaging always happens when the work function is probed at a distance which is large compared to the dimensions of the area of interest, because different net charges exist on neighboring areas of the sample if their work functions differ. To get the full local surface structure information, the surface potential has to be measured very close to the surface. It is then meaningful to define a local work function ϕ_{loc} at some point \mathbf{r} close to the surface as $\phi_{\text{loc}}(\mathbf{r}) = V_{\text{eff}}(\mathbf{r}) - E_F$,¹ where $V_{\text{eff}}(\mathbf{r})$ is the effective surface potential felt by the electron at \mathbf{r} and plays the role of a local vacuum level, and E_F is the Fermi level of the sample. Spatial variations in $V_{\text{eff}}(\mathbf{r})$ at distances of the surface of the order of 1 nm should mainly reflect either local electrostatic changes in the surface dipole layer, which saturate rapidly over few Bohr radii away from the surface, or changes in the exchange-correlation potential which is also short ranged. Local work function changes typically occur at surface inhomogeneities, e.g., at steps, impurity atoms, defects, and interfaces at patches of adsorbed species.

Experimentally, local work functions have been probed in various ways. Two spectroscopic techniques take advantage of the presence of image potential states (IPSS) at surfaces which form a Rydberg series pinned to the local vacuum level.³ In two photon photoemission (2PPE)⁴ and inverse photoemission^{5,6} experiments, IPS energies are measured with respect to E_F and the vacuum level is extracted from an interpolation of the quantum defect formula for a Rydberg series.⁷ These methods opened up the possibility to extract layer dependent work functions of homogeneous adsorbed layers.^{8–10} Whereas a usual photoemission experiment probes the work function averaged over a macroscopic sample area, photoemission of adsorbed xenon was a breakthrough because of the large diameter of a Xe atom and its weak bonding interaction with any substrate. Therefore, the surface po-

tential could be measured at about 0.2 nm in front of the surface by site-sensitive Xe atom probes distributed over the whole surface, with a lateral sensitivity of 0.5–1.0 nm.¹ Kelvin probe force microscopy¹¹ and photoemission electron microscopy¹² have shown that contact potentials can be detected on a length scale of several tens of nanometers. With the close proximity between tip and sample, scanning tunneling microscopy (STM) confirmed the existence of different local surface potentials at the atomic scale through apparent barrier height measurements.¹³ This technique is spatially sensitive to the variations of the decay length of the electron density at E_F , perpendicular to the surface. In practice, the widely used one-dimensional (1D) model of a trapezoidal barrier to approximate the tunnel barrier is a crude approximation. It neglects the tip and sample image potential contribution and requires a determination of the tip work function to extract quantitative information about the sample work function. On the other hand, after the pioneering work of Becker *et al.*¹⁴ and Binnig *et al.*,¹⁵ scanning tunneling spectroscopy (STS) of field emission resonance (FERs) was recognized to be a sensitive probe to access qualitatively local surface potential changes.^{16–20} However, quantitative analysis allowing local work function changes to be extracted has not been carried out up to now from STM or STS measurements.

In this work, we show that low temperature STS of the FERs on a metallic surface partially covered with ultrathin insulating layers allows us to extract quantitatively the local surface potential changes by a 1D model calculation. We inferred the absolute value of the adsorbate induced work function from ultraviolet photoelectron spectroscopy (UPS) measurement of the bare surface. As a particular system, we studied NaCl/Ag(100). The obtained work function equals 3.2 ± 0.1 eV on the first 3 ML (monolayer) NaCl/Ag(100). Our study shows that in order to reproduce correctly the binding energies of high-order FERs, it is necessary to take into account the shape of the tip apex. Across the edge of a NaCl island, abrupt changes occur in the energy levels of the FERs within a 1 nm wide region where tunneling into both NaCl/Ag(100) and Ag(100) occurs. This result yields a lateral resolution of 1 nm for local surface potential differences, which reflects the diameter of the effective emission area at the tip apex.

The experiments were carried out in a homebuilt scanning

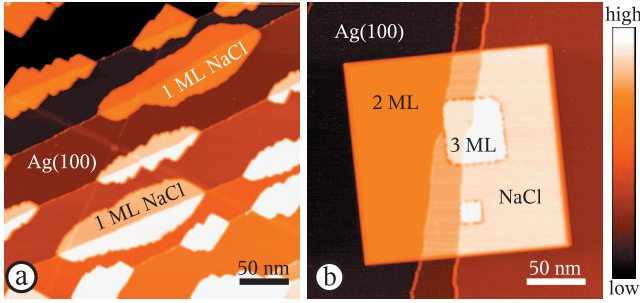


FIG. 1. (Color) STM images of NaCl grown on a Ag(100) substrate at (a) room temperature (the islands without label are 2 ML thick, $V_{\text{bias}}=4.35$ V, $I=20$ pA) and (b) 200 °C substrate temperature ($V_{\text{bias}}=4.26$ V, $I=20$ pA).

tunneling microscope²¹ operated at 50 K. The Ag(100) substrate was cleaned by Ar sputtering and subsequent annealing. The NaCl was thermally evaporated from a homebuilt evaporator at substrate temperatures ranging from room temperature to 200 °C. All dI/dV measurements were performed with closed feedback loop (constant current mode) using the lock-in technique with a modulation voltage of 5–10 mV p.p. at ~ 1.5 kHz with tunneling currents ranging from 20 to 100 pA. Simultaneously, $\Delta z(V_{\text{bias}})$, i.e., tip displacement curves were recorded. During the spectroscopic measurements on the Ag(100) substrate and on NaCl/Ag(100), care was taken of preserving identical tip conditions.

Figure 1(a) shows NaCl islands grown on a substrate at room temperature. A majority of 2 ML islands (topographic height at low V_{bias} : 310 pm) are formed and very few 1 ML islands (180 pm) are found. At higher substrate temperature, square shaped 2 and 3 ML (460 pm) islands are grown, as shown in Fig. 1(b).²²

In Fig. 2, typical dI/dV spectra together with the corresponding Δz data are presented. Prominent peaks due to the FERs are noticeable.^{14,15} Clearly visible is the difference in the voltage onset for the FERs on the clean Ag(100) and the NaCl islands. As the FERs start to appear for voltages around the sample work function,²³ this large shift toward lower energy is closely related to the difference in local work functions between the two surfaces.

However, to extract the local work function difference between two different domains on the surface, the following points are important and are incorporated into a simple 1D model for a quantitative description of the FER levels. (i) The image potential itself, which determines the IPS binding energies (at zero field), is different in the two cases. (ii) For a given voltage and tip-sample distance, the electric field in the junction is not the same in the two cases due to the presence of the dielectric layer. Therefore, the Stark effect due to the electric field between the tip and the sample shifts the FERs to different energies. (iii) As Δz varies with V_{bias} , the entire FER spectrum evolves upon the Stark effect in a nonlinear manner with V_{bias} and has no simple relation with respect to the local vacuum level of the sample, in contrast to previous assumptions.²⁴

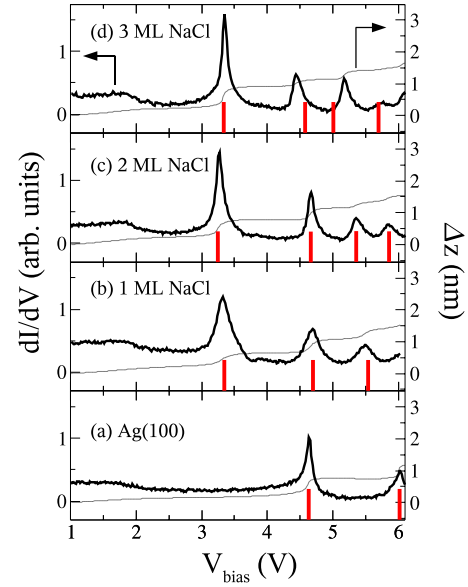


FIG. 2. (Color online) Typical dI/dV spectra (full black line). The light black line shows $\Delta z(V_{\text{bias}})$ data, i.e., the distance the tip was retracted during the dI/dV measurement. The red bars indicate the simulated FER energies.

As the IPSs are free-electron-like for electron motion parallel to the surface but localized in the direction perpendicular to the surface, our model consists of a single particle 1D Schrödinger equation in the z direction:

$$-\frac{\hbar^2}{2m} \frac{d^2 \psi(z)}{dz^2} + V(z) \psi(z) = E_n \psi(z).$$

The electronic structure of the substrate is described by a nearly free electron model (NFE) which reproduces the Ag(100) projected band gap at the known energies.^{25,26} The corresponding NFE parameters are the amplitude of the periodic potential, $V_g=2.225$ eV, and its position below $E_{F,s}$, $V_0=4.505$ eV, with a 204.5 pm period [distance between (100) planes in the Ag bulk crystal]. The Ag(100) work function is $\phi_s=4.5$ eV, as deduced from UPS experiments of the same sample, which is in good agreement with the literature.²⁷ In the probed energy range, all the observed FERs lie in the projected band gap. The electric potential between tip and sample (green in Fig. 3) is calculated by assuming a spherical tip apex of radius R .^{28,29} The image potential of the tip is taken into account.

For Ag(100), $V(z)$ consists of (i) the image potential of the sample with respect to the mirror plane at z_m (free parameter^{26,30}), which is set constant at z values where it would be below the minimum bulk potential, (ii) the image potential of the tip, and (iii) the electric potential between tip and sample. The tip-sample distance is given by the sum of the initial distance z_0 (free parameter) and $\Delta z(V_{\text{bias}})$. The Schrödinger equation for the bare surface is then solved for the eigenvalues $E_n(V_{\text{bias}})$ for every V_{bias} value and corresponding $z_0 + \Delta z(V_{\text{bias}})$ distance encountered in the experiment. The condition $E_n(V_{\text{bias}}) = E_{F,t}$, i.e., $E_n(V_{\text{bias}}) = E_{F,s} + V_{\text{bias}}$, determines the simulated FER spectrum. This first

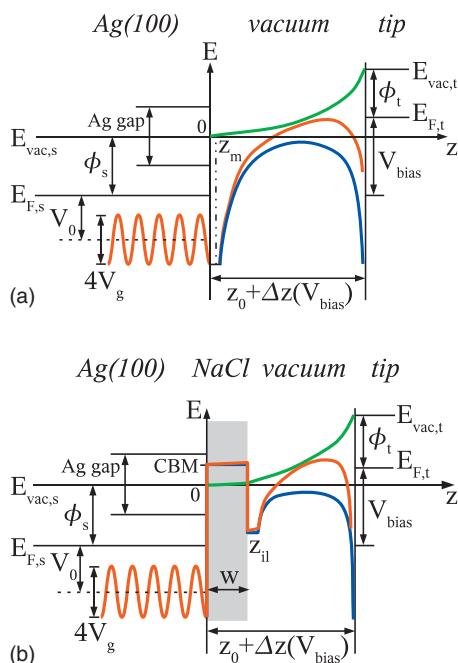


FIG. 3. (Color) Components of the $V(z)$ potential calculated to simulate the FER levels on (a) Ag(100) and (b) NaCl/Ag(100): image potential without electric field (blue), electric potential between tip and sample for an applied bias voltage V_{bias} (green), and sum of both components (red).

step allows us to extract z_0 and the tip parameters ϕ_t and R by the best fit of the calculated FERs to all the experimental dI/dV spectra measured on Ag(100) (see Fig. 2 and Table I).

The determined z_0 value is in overall agreement with values for typical tunneling resistances.³¹ The z_m value agrees well with those determined in previous work.^{25,26,30} The R value is consistent with previous calculations.³⁰

The tip parameters ϕ_t and R extracted from the measurements on the bare surface are used to simulate the FER spectrum on NaCl/Ag(100). The potential is the one previously used to interpret 2PPE experiments,^{7,32} extended by a term taking into account the electric potential between tip and sample³³ [see Fig. 3(b)]. The NaCl film is modeled by a tunnel barrier with a height equal to the conduction band minimum of bulk NaCl [0.8 eV above $E_{\text{vac},s}$ (Ref. 34)]. Its

TABLE I. Averaged parameters obtained by fitting the calculated FER spectra on the clean substrate and on the NaCl islands to the dI/dV spectra (see Fig. 2). The given uncertainties correspond to the dispersion of the extracted parameters for all fitted spectra.

Ag(100)			
R (nm)	5.6 (3 to 10)	z_m (nm)	0.015 ± 0.004
z_0 (nm)	1.17 ± 0.07	ϕ_t (eV)	4.3 ± 0.4
NaCl/Ag(100)			
	1 ML	2 ML	3 ML
ϵ	2.0 ± 0.1	3.2 ± 0.2	3.5 ± 0.1
ϕ_s (eV)	3.2 ± 0.1	3.2 ± 0.1	3.2 ± 0.1
z_0 (nm)	1.28 ± 0.04	1.48 ± 0.06	1.61 ± 0.08

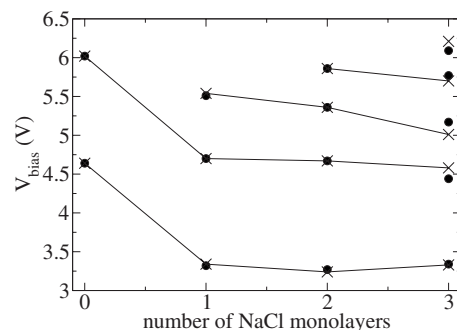


FIG. 4. Measured (dots) and calculated (crosses) FER energies as a function of NaCl coverage. The thin lines connect the calculated points.

thickness w equals the number of monolayers multiplied by 282 pm, the distance between neighboring (100) planes in bulk NaCl. The potential in the vacuum region follows the dielectric continuum model developed by Cole.³⁵ It is set constant to its value at $z_{\text{il}} = w + 0.12$ nm until it reaches the mirror plane at the dielectric-vacuum interface. The only free parameters we extract are ϵ , the dielectric constant of the NaCl layer, z_0 , the initial distance between tip and metal surface, and ϕ_s (see Table I).

Figure 2 shows very good agreement between the measured and simulated peak positions of the FERs up to 2 ML NaCl/Ag(100). The general trend between measured and calculated FER energies as a function of NaCl layer thickness is illustrated in Fig. 4. While the agreement between experiment and simulation is quantitative for the first 2 ML

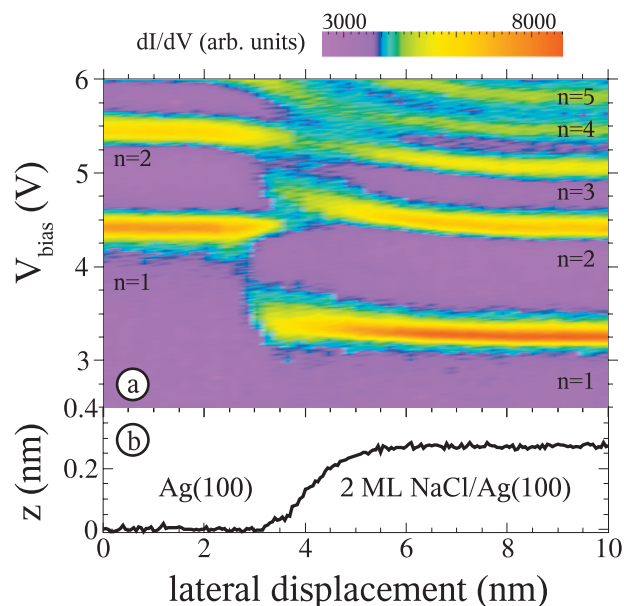


FIG. 5. (Color) (a) dI/dV spectra taken across the step edge of a 2 ML NaCl island every 0.2 nm. (b) Step profile scanned with $V_{\text{bias}} = 0.2$ V, $I = 20$ pA. The island step edge is laterally offset by about 0.8 nm between topography (b) and FERs (a) as a consequence of the finite emission area of the tip. Note the bending of the FER energies over a length of ~ 7 nm as a consequence of the local lateral contact potential.

of NaCl on Ag(100), it becomes only qualitative for 3 ML of NaCl. A similar irregular behavior in the simulation of IPS has been observed in a 2PPE experiment at zero external field by McNeill *et al.*,³² where an equivalent model was applied to simulate the IPS spectrum up to nine layers of Xe on Ag(111). McNeill *et al.* found that in their model for a coverage of 5 ML of Xe, the energy difference between the second and the third IPS becomes larger than the one between the first and the second IPS. In our case of an STM junction, the model has to include the electric field between the tip and the sample, which, in the simulation, pushes the FERs toward the sample surface.³⁶ As a consequence, the model shows this irregularity in the energy spacing already at a coverage of 3 ML NaCl. Here, the contribution of the dielectric layer to the total potential in the junction makes the total potential deviate significantly from the central Coulomb potential or from a triangular potential well. Evidently, our simple model does not account for the influence of the atomic potentials of the NaCl layers on the FER wave functions with a significant weight inside the dielectric layer.

The parameter ϵ (Table I) turns out to be smaller than the NaCl bulk value of 5.9 (Ref. 37) and increases with layer thickness as confirmed by a local field model.³⁸ After formation of 1 ML islands, the work function is found to be decreased by 1.3 eV and stays constant for additional NaCl layers. A UPS measurement of the work function as a function of the NaCl coverage yields a value of 3.5 ± 0.1 eV at saturation coverage. The difference of about 0.3 eV between the local STS measurement on an individual NaCl island and the macroscopic UPS measurement on a sample surface with

varying morphology is ascribed to the inherent averaging over the probed sample area in UPS, yielding an upper limit for the work function. Our results are consistent with 2PPE results on various rare gas adlayers on Cu(100), showing that the major drop in ϕ occurs after deposition of 1 ML.⁷ However, the reduction of ϕ for ionic adlayers is stronger than for rare gas adlayers where the change is below 0.5 eV.

Figure 5 shows laterally resolved STS of FERs taken across the step edge of a NaCl island of 2 ML height. A discontinuous transition in the first FER energy is observed at the lateral interface between Ag(100) and NaCl/Ag(100), reflecting the lateral surface potential change on the nanoscale. The fact that transmission into the two characteristic FERs above both types of surfaces extends over a lateral range of 1 nm indicates an emission area of the tip apex of ~ 1.5 nm², which determines the finite lateral resolution of the measurement. This value is in agreement with emission area calculations³⁰ when extrapolated to $R=5.6$ nm (see Table I).

In conclusion, measurements of FERs with STS in combination with a calculation based on a simple 1D model of the potential well between tip and sample yield the local work function changes between a Ag(100) substrate and ultrathin dielectric NaCl islands of different heights grown on Ag(100). This method spatially maps the local work function changes with a typical lateral resolution of 1 nm. Possible applications abound, e.g., in thin film characterization, adsorption, reactions, and nanocatalysis.

The financial support of the Swiss National Science Foundation is gratefully acknowledged.

-
- ¹K. Wandelt, in *Thin Metal Films and Gas Chemisorption*, edited by P. Wissmann (Elsevier, Amsterdam, 1987), Chap. 7, p. 280.
- ²D. P. Woodruff and T. A. Delchar, *Modern Techniques of Surface Science*, 2nd Edition (Cambridge University Press, Cambridge, UK, 1994).
- ³P. M. Echenique and J. B. Pendry, *J. Phys. C* **11**, 2065 (1978).
- ⁴K. Giesen, F. Hage, F. J. Himpsel, H. J. Riess, and W. Steinmann, *Phys. Rev. Lett.* **55**, 300 (1985).
- ⁵V. Dose, W. Altmann, A. Goldmann, U. Kolac, and J. Rogozik, *Phys. Rev. Lett.* **52**, 1919 (1984).
- ⁶D. Straub and F. J. Himpsel, *Phys. Rev. Lett.* **52**, 1922 (1984).
- ⁷W. Berthold, F. Rebrost, P. Feulner, and U. Höfer, *Appl. Phys. A: Mater. Sci. Process.* **78**, 131 (2004).
- ⁸D. F. Padowitz, W. R. Merry, R. E. Jordan, and C. B. Harris, *Phys. Rev. Lett.* **69**, 3583 (1992).
- ⁹M. Donath and K. Ertl, *Surf. Sci.* **262**, L49 (1992).
- ¹⁰R. Fischer, S. Schuppler, N. Fischer, T. Fauster, and W. Steinmann, *Phys. Rev. Lett.* **70**, 654 (1993).
- ¹¹J. M. R. Weaver and D. W. Abraham, *J. Vac. Sci. Technol. B* **9**, 1559 (1991).
- ¹²H. Bethge and M. Klaua, *Ultramicroscopy* **11**, 207 (1983).
- ¹³L. Olesen, E. Lægsgaard, I. Stensgaard, and F. Besenbacher, *Appl. Phys. A: Mater. Sci. Process.* **66**, S157 (1998), and reference therein.
- ¹⁴R. S. Becker, J. A. Golovchenko, and B. S. Swartztruber, *Phys. Rev. Lett.* **55**, 987 (1985).
- ¹⁵G. Binnig, K. H. Frank, H. Fuchs, N. Garcia, B. Reihl, H. Rohrer, F. Salvan, and A. R. Williams, *Phys. Rev. Lett.* **55**, 991 (1985).
- ¹⁶T. Jung, Y. W. Mo, and F. J. Himpsel, *Phys. Rev. Lett.* **74**, 1641 (1995).
- ¹⁷E. D. L. Rienks, N. Nilius, H.-P. Rust, and H.-J. Freund, *Phys. Rev. B* **71**, 241404(R) (2005).
- ¹⁸D. B. Dougherty, P. Maksymovych, J. Lee, and J. T. Yates, Jr., *Phys. Rev. Lett.* **97**, 236806 (2006).
- ¹⁹A. Kubetzka, M. Bode, and R. Wiesendanger, *Appl. Phys. Lett.* **91**, 012508 (2007).
- ²⁰A. Hanuschkin, D. Wortmann, and S. Blügel, *Phys. Rev. B* **76**, 165417 (2007).
- ²¹R. Gaisch, J. K. Gimzewski, B. Reihl, R. R. Schlittler, M. Tschudy, and W.-D. Schneider, *Ultramicroscopy* **42**, 1621 (1992).
- ²²M. Pivetta, F. Patthey, M. Stengel, A. Baldereschi, and W.-D. Schneider, *Phys. Rev. B* **72**, 115404 (2005).
- ²³K. H. Gundlach, *Solid-State Electron.* **9**, 949 (1966).
- ²⁴P. Wahl, M. A. Schneider, L. Diekhöner, R. Vogelgesang, and K. Kern, *Phys. Rev. Lett.* **91**, 106802 (2003).
- ²⁵N. V. Smith, C. T. Chen, and M. Weinert, *Phys. Rev. B* **40**, 7565 (1989).
- ²⁶M. Ortuño and P. M. Echenique, *Phys. Rev. B* **34**, 5199 (1986).
- ²⁷S. Schuppler, N. Fischer, T. Fauster, and W. Steinmann, *Appl. Phys. A: Solids Surf.* **51**, 322 (1990).

- ²⁸W. R. Smythe, *Static and Dynamic Electricity*, International Series in Pure and Applied Physics (McGraw-Hill, New York, 1968).
- ²⁹Our calculations show that the plane electrode approximation for the tip is not appropriate to describe correctly high-order FERs because the tip-sample distance is not negligible anymore compared to R .
- ³⁰J. M. Pitarke, F. Flores, and P. M. Echenique, *Surf. Sci.* **234**, 1 (1990).
- ³¹J. K. Gimzewski and R. Möller, *Phys. Rev. B* **36**, 1284 (1987).
- ³²J. D. McNeill, J. R. L. Lingle, R. E. Jordan, D. F. Padowitz, and C. B. Harris, *J. Chem. Phys.* **105**, 3883 (1996).
- ³³B. Techaumnat and T. Takuma, *IEEE Trans. Dielectr. Electr. Insul.* **13**, 336 (2006).
- ³⁴R. C. Leckey, in *Condensed Matter*, edited by A. Goldmann and E.-E. Koch, Landolt-Börnstein, New Series, Group III, Vol. 23, Pt. A (Springer-Verlag, 2006), p. 113.
- ³⁵M. W. Cole, *Phys. Rev. B* **3**, 4418 (1971).
- ³⁶S. Crampin, *Phys. Rev. Lett.* **95**, 046801 (2005).
- ³⁷M. Robinson and A. H. Hallett, *Can. J. Phys.* **44**, 2211 (1966).
- ³⁸K. Natori, D. Otani, and N. Sano, *Appl. Phys. Lett.* **73**, 632 (1998).